General Synthesis of a Mesoporous Composite of Metal Oxide and Silicate Nanoparticles from a Metal Salt and Laponite Suspension for Catalysis

H. Y. Zhu,*[,†] J.-C. Zhao,[‡] J. W. Liu,[†] X. Z. Yang,[†,§] and Y. N. Shen [§]

Inorganic Materials Research Program, School of Physical and Chemical Sciences, Queensland University of Technology, GPO Box 2434, Brisbane, QLD 4001 Australia, Centre for Molecular Science, Institute of Chemistry, The Chinese Academy of Science, Beijing 100080, China, and College of Chemistry and Chemical Engineering, Inner Mongolia University, Huhhot, 010021, People's Republic of China

Received February 16, 2006. Revised Manuscript Received May 1, 2006

A general approach is proposed for the synthesis of thermally stable and highly porous composite structures of metal oxide and silicate nanoparticles from aqueous solution of a metal salt and a suspension of Laponite clay. The formation of the mesoporous structure involves coupled processes: acid leaching of the Laponite clay sheets by acidic aqueous solution of the metal salt and polymerization of the metal hydrate species due to the high pH of the Laponite suspension. The extent of the acid leaching varies with the acidity of the metal salt solution. Moreover, introducing poly(ethylene oxide) surfactants in the synthesis significantly increases surface areas and porosity of the products. The nanocomposites obtained possess large porosity, large accessible surface area of metal oxide nanocrystals, and ion exchange capacity. They can be readily granulated, and metals can be loaded onto the solids by ion exchange and exist in highly dispersed metal nanocrystals. They have been found to be superior photocatalysts or supports for metal catalysts. The reaction mechanism of the synthesis is distinctly different from that for the synthesis of conventional pillared intercalated layered clays. This synthesis approach is an effective approach for constructing nanocomposites with a large porosity and structure and surface chemistry that can be tailored.

Introduction

Transition metal oxides are widely used as catalysts or catalyst supports.[1−3] The fine particles of transition metal oxides, with particle sizes in a range of several nanometers, are particularly attractive materials because these nanoparticles have a large specific surface area on which the catalytic reaction takes place and often exhibit superior catalytic properties. However, the synthesis of metal oxide nanoparticles is relatively complicated and costly.[3] In many cases, heating at high temperature is necessary during the preparation to convert metal hydrate or hydroxides to oxides, but sintering of the fine particles during heating is inevitable and results in large particles with small surface areas. Because the catalytic reactions take place on the surface of the catalysts, the reaction rates are in proportion to the surface area of the catalysts. To achieve thermally stable structures with a large surface area of the transition metal oxides, creating porous composite structures is a feasible option. In such structures, the fine particles of metal oxides are dispersed within an inorganic media (the second component) on the scale of nanometers. The second component partitions the fine metal oxide particles and prevents them from sintering so that the metal oxide can still exist as nanoparticles after heating and retains a large surface area. The reactant molecules can access and react on the surface of the metal oxide through the pores in the composites. Actually, in the pillared layered clays developed in the late 1970s,[4−7] the clay layers act as such an inorganic media. The clay layers are about 1 nm thick and carry negative electric charges.[8] There are charge-balancing cations between the layers. Polymerized cations or positively charged sol particles of metal hydrate, $[MO(OH)_x]_m^{n+}$, prepared readily from inorganic salts, can replace the interlayer cations by an ion exchange process.[4−7,9,10] They are converted to oxide pillars after being heated to above 400 °C, propping the clay layers apart. The metal oxide pillars are small (<2 nm) and are generally amorphous particles.[9,10] It is extremely difficult to obtain large pillar precursors without precipitation in the conventional pillaring process. This problem seriously limits their applications. For instance, a crystallite form of TiO_2, in an anatase or rutile phase, is necessary for an efficient photocatalyst. However, the TiO_2 pillars in the conventional

* Corresponding author. E-mail: hy.zhu@qut.edu.au and fax: 61 7 3864 1804.
† Queensland University of Technology.
‡ The Chinese Academy of Science.
§ Inner Mongolia University.

(1) Rao, C. N. R.; Raveau, B. *Transition Metal Oxides*, 2nd ed.; Wiley-VCH: New York, 1998.
(2) Jolivet, J.-P. *Metal Oxide Chemistry and Synthesis: From Solution to Solid State*; Wiley: New York, 2003.
(3) Seshan, K.; Barge, H. M.; Hally, W.; Keulen A. N. J.; Joss, J. R. H. *Stud. Surf. Sci. Catal.* **1994**, *81*, 285.
(4) Brindley, G. W. *Clay Miner.* **1977**, *12*, 229.
(5) Lahav, N.; Shani, U.; Shabtai, J. *Clays Clay Miner.* **1978**, *26*, 19.
(6) Yamanaka, S. *Clays Clay Miner.* **1979**, *27*, 119.
(7) Vaughan, D. E. W.; Lussier, R. J. In *Proceedings of the 5th International Conference on Zeolites*; Rees, Lovat, V. C., Eds.; Heyden: London, 1980; p 94.
(8) Newman, A. C. D. *Chemistry of Clays and Clay Minerals*; Longmans: London, 1987.
(9) Burch, R., Ed. *Pillared Clays, Catalysis Today*; Elsevier: New York, 1988; Vols. 2 and 3.
(10) Pinnavaia, T. J. *Science* **1983**, *220*, 365.

10.1021/cm060390+ CCC: $33.50
Published on Web 07/18/2006

TiO_2 pillared clays are too small to form crystallites, and the pore size of these pillared clays, which is associated with the pillar size, is too small to allow the large organic molecules to diffuse quickly to the pillar surface. The poor activity of amorphous TiO_2 pillars and the diffusion difficulty make the TiO_2 pillared clays exhibit a moderate catalytic performance for photodegradation of organic pollutants that are usually large molecules.[11] It is known that interlayer pores of alumina pillared clays are about 0.7−0.8 nm.[4,5,7,9] However, after loading transition metal ions by a cation exchange process, these interlayer pores were almost blocked, losing most of their nitrogen adsorption capacity.[12,13] It means that when the solid is used as a catalyst support, loaded metal ions or metal atom clusters will block interlayer pores, and the active component in the pores becomes inaccessible to most reactant molecules. Besides, for many reactions, the diffusion of reactant and product molecules is a more serious concern than a molecular sieving effect. Under these circumstances, the diffusion of molecules in the two-dimensional pore system of pillared clays is depressed and may cause problems, like coking, and the catalysts lose activity in a short period.[14] Actually, the applications of the pillared clays as catalysts and catalyst supports have been seriously impeded by these problems.

For applications as catalysts and catalyst supports, mesoporous structures are desired.[15] In such structures, a metal oxide can exist as a crystallite of several nanometers. One can also load an active component into the mesoporous structures without blocking the pores, so that the surface of the metal oxide is still accessible to the reactant molecules after the loading. One merit of pillared clays is that the clay layers partition the metal oxide pillars, preventing them from sintering. The losses of the porosity and specific surface area of the pillared clays during heating at high temperatures are usually due to the collapse of the clay layers rather than sintering of the pillars.[16] Thus, mesoporous composites of metal oxide nanocrystals and silicate are optimal structures for catalysis materials if we can invent new and viable synthesis techniques for mesoporous composites. In previous papers, we noted that mesoporous composite structures of silicate and titanium dioxide[17] or silicate and zirconium oxide[18] could be created by the reaction between a titanium sol and a Laponite suspension or between a zirconium salt solution and a Laponite suspension.

Hydrate cations of many metal elements are stable in an acidic environment.[2,19] If the pH increases, the metal hydrate cations will hydrolyze, forming polymerized hydrate ions (oligomers), and finally precipitate. Actually, the dispersion of Laponite, a synthetic clay which is isostructural with smectite clays, has a pH of about 10. This pH is effective for inducing further hydrolysis of the oligomers of various metal hydrates. The clay platelets are small, about 30 nm in diameter.[20] In a dilute aqueous dispersion, the clay exists as discrete plates.

In the present study, we report a generalized synthesis of highly porous composite structures of metal oxide and silicate particulates, which are several nanometers in size, from aqueous solutions of metal salts and dispersion of Laponite clay. This synthesis is distinctly different, in terms of reaction mechanisms, from the conventional pillaring process[4−7,9,10] and the synthesis of porous clay heterostructures (PCHs).[21] In the conventional synthesis of pillared clays and PCHs, the clay layers are retained intact. On the contrary, the synthesis approach of this study is designed to strengthen the reaction between the Laponite clay and the pillaring solution to create mesoporous structures rather than microporous solids such as pillared clays. It involves coupled processes: the hydrolysis of the metal hydrate species due to the high pH of the clay suspension and acid leaching of the clay sheets by the acidic solution of metal hydrates. As expected, the mesoporous composites obtained exhibit superior catalytic performance and thermal stability to the microporous counterpart pillared clays.

Experimental Procedures

Materials. The Laponite clay (Laponite RD) was supplied by Fernz Specialty Chemicals, Australia and used as received. The clay powder has a BET specific surface area of 370 m^2/g and a cation exchange capacity of 55 meq per 100 g of clay. The chemicals used as the source of metal oxides, such as $Fe(NO_3)_3 \cdot 9H_2O$, $ZrOCl_2 \cdot 8H_2O$, $Cr(NO_3)_3 \cdot 9H_2O$, $MnSO_4 \cdot 6H_2O$, $Ni(NO_3)_2 \cdot 6H_2O$, $CeCl_3 \cdot 7H_2O$, and titanium tetraisopropoxide $Ti(OC_3H_7)_4$, etc., were AR grade and purchased from Aldrich. They were used as received without further purification. Nonionic poly(ethylene oxide), PEO, surfactants from Aldrich, with a trade name Tergitol 15S-*n* ($n = 5$, 7, 9, 12, and 30), were used in this study as a spacer to increase the porosity in the products. The PEO surfactants have a general chemical formula of $C_{12-14}H_{25-29}O(CH_2CH_2O)_nH$ and have relatively small average molecular weights. For example, the molecular weights of Tergitol 15S-5 ($n = 5$) and Tergitol 15S-12 ($n = 12$) are 420 and 730 g/mol, respectively.

Preparation of Samples. The aqueous pillaring solutions in conventional pillared clay synthesis were prepared and used as the sources of the metal oxides. The sol solution of titanium hydrate was prepared by the hydrolysis of $Ti(OC_3H_7)_4$ in HCl solution and aged for 3 h,[22,23] following the procedures proposed by Yamanaka et al.[23] The molar ratio of $[Ti]/[H^+]$ is 1:4. The solution containing oligomers of iron hydrate was obtained by adding 4.66 g of sodium carbonate (Na_2CO_3) slowly as a powder into the vigorously stirred solution of a 0.2 M iron(III) nitrate solution. The molar ratio of base to Fe $[Na^+]/[Fe^{3+}]$ was 1:1. The pillaring solution thus obtained was stirred for 3 h and used as an iron oxide precursor. An aqueous

(11) Yoneyama, H.; Haga, S.; Yamanaka, S. *J. Phys. Chem.* **1989**, *93*, 4833.
(12) Zhu, H. Y.; Yamanaka, S. *J. Chem. Soc., Faraday Trans.* **1997**, *93*, 477.
(13) Zhu, H. Y.; Zhu, Z. H.; Lu, G. Q. *J. Phys. Chem.* **2000**, *104*, 5674.
(14) Wang, S. B.; Zhu, H. Y.; Lu, G. Q. *J. Colloid Interface Sci.* **1998**, *204*, 128.
(15) Gil, A.; Gandia, L. M.; Vicente, M. A. *Catal. Rev.* **2000**, *42* (1 and 2), 145.
(16) Zhu, H. Y.; Xia, J. A.; Vansant, E. F.; Lu, G. Q. *J. Porous Mater.* **1997**, *4*, 17.
(17) Zhu, H. Y.; Orthman, J.; Li, J.-Y.; Zhao, J.-C.; Churchman, G. J.; Vansant, E. F. *Chem. Mater.* **2002**, *14*, 5037.
(18) Zhu, H. Y.; Hao, Z. P.; Barry, J. *Chem. Commun.* **2002**, 2858.
(19) Baes, C. F.; Mesmer, R. E. *The Hydrolysis of Cations*; J. Wiley and Sons: New York, 1986.
(20) Thompson, D. W.; Butterworth, J. T. *J. Colloid Interface Sci.* **1992**, *151*, 236.
(21) Galarneau, A.; Barodawalla A.; Pinnavaia, T. J. *Nature* **1995**, *374*, 529.
(22) Sterte, J. *Clays Clay Miner.* **1986,** *34*, 658.
(23) Yamanaka, S.; Nishihara, T.; Hattori, M.; Suzuki, Y. *Mater. Chem. Phys.* **1987**, *17*, 87.

solution of 0.5 M $ZrOCl_2$ was refluxed for a few hours and used as precursor of ZrO_2, which contains zirconium hydroxyl oligomers.[24] To prepare a mixed oxide precursor of ceria and zirconia, CeO_2/ZrO_2, a solution containing hydroxyl oligomers of zirconium and cerium with a molar ratio of Ce/Zr = 1:10 was refluxed for 2 days and used. The precursor solutions for mixed oxides of lanthanum and aluminum, and of cerium and alumium (La_2O_3/Al_2O_3 and CeO_2/Al_2O_3, respectively), were prepared following the method of Sterte[25] and our previous work:[16] a solution containing hydroxyl oligomers of aluminum (so-called Keggion ions Al_{13}) and lanthanum ions (or cerium ions) with a molar ratio of rare earth to aluminum 1:5 was refluxed for 4 days. A 0.1 M chromium(III) nitrate solution was obtained by dissolving 35.2 g of chromium nitrate, $Cr(NO_3)_3 \cdot 9H_2O$ in 426 mL of hot water (95 °C) and was used as precursor to prepare the Cr_2O_3−nanocomposite. The 0.02 M $MnSO_4$ and 0.24 M $Ni(NO_3)_2$ solutions were used directly as precursor solutions to synthesize Mn_3O_4− and NiO−nanocomposites, respectively.

A total of 4.0 g of Laponite was dispersed slowly into 200 mL of water where the suspension was stirred until it became transparent (approximately 40 min). A total of 16.0 g of a PEO surfactant was added into the Laponite dispersion to cause it to become opaque. To this mixture, a precursor solution (pillaring solution) prepared as described previously was added dropwise with continuous stirring. After stirring for 3 h, the suspension was transferred into an autoclave and maintained at 373 K for 2 days. A precipitate was recovered from the mixture by centrifuging and washed with deionized water until it was free of Cl^- ions according to a test with $AgNO_3$. The wet cake was dried in air and calcined at 773 K for 20 h. The temperature was raised at a rate of 2 K/min. The samples were labeled M_nO_m−nanocomposite (M denotes the metal element and *m* and *n* are integers)

Characterization. Transmission electron microscopy (TEM) images were taken with a JEOL 2010 microscope employing an accelerating voltage of 200 kV. The composition of some samples was determined by energy-dispersive X-ray spectroscopy (EDS) attached on the same microscope. The specimens were sample powders deposited onto a copper microgrid coated with a holey carbon film. X-ray diffraction (XRD) patterns of the sample powder were recorded on a Siemens D5000 diffractometer equipped with a graphite monochromator. Cu K_α radiation and a fixed power source (40 kV and 40 mA) were used. The data were collected over a 2θ range between 2 and 70°, at a scanning rate of 0.15°/min. N_2 adsorption/desorption isotherms were measured at a liquid nitrogen temperature using a gas sorption analyzer (Autosorb-1 Quantachrome). The samples were degassed at 523 K and under a vacuum below 10^{-3} Torr for 16 h prior to the measurement. The specific surface area was calculated by the BET equation,[26] and the pore size distribution was derived from the adsorption data.[27] Solid state ^{29}Si magic-angle spinning nuclear magnetic resonances (^{29}Si MAS NMR) were recorded at 59.63 MHz on a Bruker MSL 300 spectrometer. Powder samples were spun at a frequency of 2.5 Hz in Bruker double-air-bearing probes. The CP contact time used in this study was 8 ms.

Results and Discussion

Generally, an aqueous solution of metal hydrate species or positively charged sol particles (precursor solutions) was added into the dispersion of Laponite. The reaction mixture of the Laponite suspension and precursor solution was aged at 373 K for 2 days. This procedure is different from that in the synthesis of pillared clays, in which the reaction system is usually kept at room temperature.[4−7,9−14,16] Such an aging approach can intensify the reaction between Laponite and precursor solution because the acid leaching of layered clays is conducted at 100 °C or above.[28−30] Meanwhile, at elevated temperatures, the polycations or sol particles are prone to polymerize even further without the pH increase caused by the Laponite suspension. The metal hydrate species should hydrolyze onto the leached Laponite layers, forming a homogeneous composite in which both components have nanometer scale sizes. During subsequent calcination at 773 K, the metal hydrate species are converted to oxide nanoparticles, and robust porous composite structures of metal oxide and silicate particles are thus achieved.

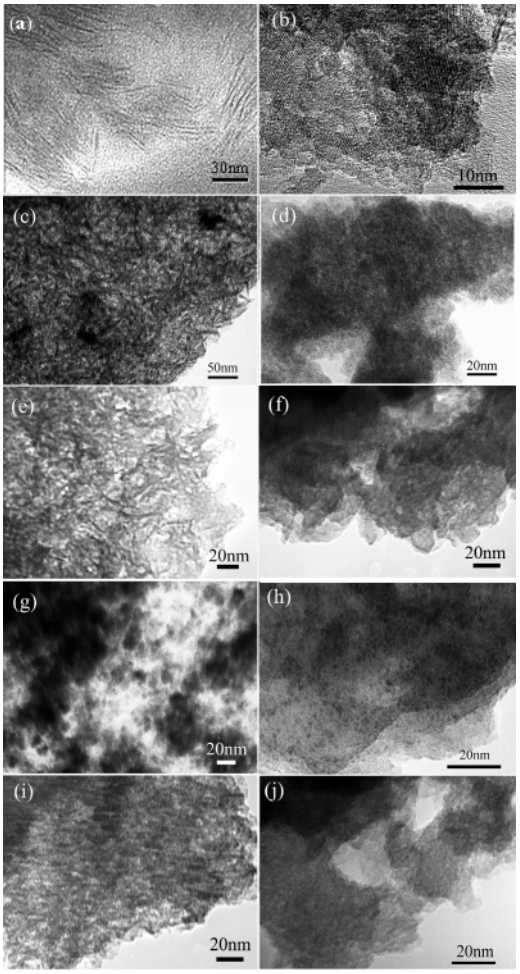

Figure 1. Transmission electron microscopy images of Laponite clay (a), TiO_2−composite (b), Mn_3O_4−composite (c), ZrO_2−composite (d), CeO_2/Al_2O_3−composite (e), La_2O_3/Al_2O_3−composite (f), Fe_2O_3−composite (g), NiO−composite (h), CeO_2/ZrO_2−composite (i), and Cr_2O_3−composite (j). The scale bars are given in the images.

The transmission electron microscopy (TEM) images of pristine Laponite and the product composites are illustrated in Figure 1. The Laponite specimen was prepared specifically to show the section of clay sheets that have a uniform

(24) Ohtsuka, K.; Hayashi, Y.; Suda, M. *Chem. Mater.* **1993**, *5*, 1823.
(25) Sterte, J. *Clays Clay Miner.* **1991**, *39*, 167.
(26) Gregg, S. J.; Sing, K. S. W. *Adsorption, Surface Area, and Porosity*, 2nd ed.; Academic Press: New York, 1982; Ch. 3.
(27) Zhu, H. Y.; Cool, P.; Vansant, E. F.; Su, B. L.; Gao, X. P. *Langmuir* **2004**, *20*, 10115.
(28) Corma, A.; Mifsud, A.; Sanz, E. *Clay Miner.* **1987**, *22* (2), 225.
(29) Mokaya, R.; Jones, W. *J. Catal.* **1995**, *153* (1), 76.
(30) Kaviratna, H.; Pinnavaia, T. J. *Clays Clay Miner.* **1994,** *42* (6), 717.

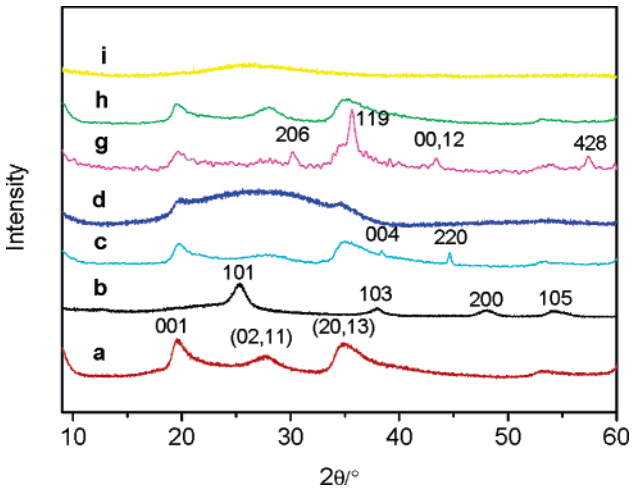

Figure 2. X-ray diffraction (XRD) patterns of some samples. The pattern of a sample is denoted by the same letter that denotes the image of the sample in Figure 1. (a) Laponite clay, (b) TiO_2−composite, (c) Mn_3O_4−composite, (d) ZrO_2−composite, (g) Fe_2O_3−composite, (h) NiO−composite, and (i) CeO_2/ZrO_2−composite. The indexed peaks on pattern b are from anatase; those on pattern c are from Mn_3O_4; and those on pattern g are from Fe_2O_3. The patterns of other samples are given in Supporting Information Figure S1.

thickness of ∼1 nm (Figure 1a). The structures of the composite samples are distinctly different from pillared clays, with no intercalated parallel layers observed. Obviously, the structures depend on the transition metal element in the samples. This is the result of the reaction between Laponite platelets and acidic solution of the metal salts. The acidity of the precursor solution varies from element to element. Curved sheets can be seen in the Mn_3O_4−nanocomposite (Figure 1c), suggesting that the clay layers have not been seriously damaged. The spongelike structure with a large porosity of a CeO_2/ZrO_2−nanocomposite (Figure 1i) results from the serious reaction that destroys clay layers in the synthesis. Similar situations are observed for the TiO_2−nanocomposite (Figure 1b), ZrO_2–nanocomposite (Figure 1d), and Cr_2O_3−nanocomposite (Figure 1j). We can see the particles with fringes in the image of the TiO_2−nanocomposite, which are anatase crystals, but no layered clays can be seen. In the images of the CeO_2/Al_2O_3−composite (Figure 1e) and La_2O_3/Al_2O_3−composite (Figure 1f), it is hard to find clay plates and alumina crystals. The clay layers could be damaged in the synthesis, and the content of the rare earth oxide is too low to observe their crystals. Under the synthesis conditions, γ-alumina, which is not a well-crystallized solid, should form. Therefore, these two samples appear analogous to porous amorphous solids. The images of the Fe_2O_3−composite (Figure 1g) and NiO−composite (Figure 1h) have features similar to Figures 1e,f. In these samples, very small metal oxide particles and silicate particles (from the damaged clay layers) are well-dispersed among each other.

The XRD patterns of some samples and Laponite clay are given in Figure 2. The diffractions from Laponite are indexed following ref 31. These diffractions are very weak or are not observed in the patterns of the CeO_2/ZrO_2–nanocomposite, TiO_2−nanocomposite, ZrO_2−nanocomposite, and Cr_2O_3−nanocomposite, indicating that the clay layers were seriously damaged or destroyed. Nonetheless, silica (SiO_2) accounts for at least 25% of the mass of the composite samples (Table 1). SiO_2 should exist in these samples in amorphous silicate nanoparticles dispersed among the metal oxide particles. The diffractions from the Laponite are observed clearly in the patterns of other samples, indicating that Laponite clay layers are retained. This can be explained by the fact that the acidity of the precursor (metal salt) solutions used in the synthesis are not strong enough to cause serious leaching and damage of the clay layer. Such an argument is supported by the data in Table 1. The MgO content in the TiO_2−, ZrO_2−, Cr_2O_3−, and CeO_2/ZrO_2−nanocomposite samples is obviously smaller, as compared with that in the pristine Laponite. Most of the magnesium in the Laponite platelets is leached out by the sol of titanium(IV) hydrate, the solutions containing hydroxyl oligomers of zirconium, and the oligomers of zirconium and cerium hydrate. The Laponite clays consist of an octahedral MO_6 layer sandwiched between two tetrahedral SiO_4 layers.[8] Magnesium atoms are at the center of the MO_6 octahedra. When the magnesium in the Laponite clay is leached out, the residue left in the samples is more likely amorphous silicate particles as reaction products. The content of MgO in the samples is, therefore, indicative of the acid leaching by the precursor solutions used in the syntheses. A substantial loss of magnesium implies the damage of clay layers. As can be seen, for the samples having a substantial low MgO content, there are no or very weak diffractions from Laponite in their XRD patterns. On the other hand, the XRD patterns in Figure 2 also indicate the existence of some metal oxide crystals in the corresponding samples: anatase in the TiO_2−nanocomposite, Fe_2O_3 in the Fe_2O_3−nanocomposite, and Mn_3O_4 in the Mn_3O_4−nanocomposite. The peaks from these oxides are indexed on the corresponding patterns. Dark-field images of some samples are provided in Figure S1 of the Supporting Information. The images formed from diffraction beams while the transmitted beam was blocked. The bright spots are crystals that orient in the right direction so that the diffraction beam scattered from them can generate the image. The images confirm the existence of metal oxide nanocrystals. For other samples, no diffractions from metal oxide crystals can be clearly observed. This could be due to the metal oxide particles in these samples having a poor crystallinity. The XRD patterns of the CeO_2/Al_2O_3−composite, La_2O_3/Al_2O_3−composite, and Cr_2O_3–composite samples have a similar appearance to that of the Mn_3O_4−

Table 1. Major Chemical Composition of Some Composite Samples Determined by EDS

sample	SiO_2 (%)	Al_2O_3 (%)	MgO (%)	TiO_2 (%)	Na_2O (%)	Fe_2O_3 (%)	Cr_2O_3 (%)	ZrO_2 (%)
laponite	51.10	0.07	23.20	*a*	2.51			
ZrO_2−C[b]	40.02	0.20	3.44			0.14		33.20
TiO_2−C	42.58	0.09	0.14	33.88		0.01		
Fe_2O_3−C	33.53	0.01	16.40			23.71		
Cr_2O_3−C	25.71	0.01	4.65				47.20	
NiO−C	41.01	0.01	14.96				23.20 (NiO)	
Mn_3O_4−C	44.11	0.01	21.30				9.91 (MnO_2)	
ZrO_2/CeO_2−C	37.73	0.21	3.54				0.52 (CeO_2)	33.11
Al_2O_3/ CeO_2−C	39.72	20.89	15.81				0.57 (CeO_2)	
$Al_2O_3La_2O_3$−C	37.94	21.24	17.19				0.35 (La_2O_3)	

[a] Not detectable. [b] C is an abbreviation of the composite in this table so that ZrO_2−C is ZrO_2−composite (the same for the other samples).

(31) Qi, Y.; A1-Mukhtar, M.; Alcover, J.-F.; Bergaya, F. *Appl. Clay Sci.* **1996**, *11*, 185.

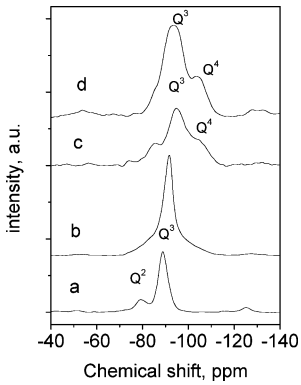

Figure 3. ^{29}Si magic-angle spinning nuclear magnetic resonance (^{29}Si MAS NMR) of the samples. Spectrum a is the spectrum for Laponite clay; spectrum b, for Al_2O_3−composite; spectrum c, for TiO_2−composite; and spectrum d, for the Cr_2O_3−composite with a low Cr_2O_3 content.

composite, except that there are no 004 and 220 diffraction peaks of Mn_3O_4. These patterns are given in Figure S2 of the Supporting Information.

It has been known that some layered clays can react with various acids even at moderate conditions.[28−30] But, this phenomenon has been ignored in the synthesis of pillared clays, and the clay layers are regarded as inert and retain their intact layer structure during the synthesis.[4−7,21−24] The conventional synthesis of pillared clays is usually carried out at ambient temperature at which the acid leaching could be regarded as negligible if a neutral clay with a more rigid structure, like montmorillonite, is used. Nonetheless, given the fact that the pH of the synthetic Laponite suspension is about 10, when Laponite is used and the reaction mixtures are aged at higher temperatures (373 K), the acid leaching is greatly promoted. The acid leaching of the clay layers benefits from the aging at high temperatures.[28−30]

The results of ^{29}Si magic-angle spinning nuclear magnetic resonance (^{29}Si MAS NMR) of the samples (Figure 3) also confirm the acid leaching reaction during the synthesis. The NMR spectra indicate the different structure changes in silicate platelets caused by the reaction.

^{29}Si MAS NMR spectrum of Laponite displays two resonance peaks at −90 and −80 ppm. Such chemical shifts are correlated to the SiO_4 tetrahedras linked with three and two other SiO_4 tetrahedras (Q^3 and Q^2 sites), respectively. This is expected for the structure of a Laponite clay layer.[8,32] In the clay layer, most SiO_4 tetrahedras are linked to three other SiO_4 tetrahedra and form the Q^3 sites, but the tetrahedra at the edges of the clay layers are linked to two other SiO_4 tetrahedra and thus form the Q^2 sites. The smaller amount of Q^2 sites, as compared to that of the Q^3 sites, is responsible for the low intensity of the peak at −80 ppm.

The TiO_2−composite and Cr_2O_3−composite samples show substantially different MAS NMR spectra. Broad resonance in the range from −110 to −80 ppm can be seen, reflecting poor short-range order. It also suggests a radical structure change of the silicate due to the reaction in the synthesis. The chemical shift at −104 ppm (a peak for the Cr_2O_3−composite and a shoulder for the TiO_2−composite) should be assigned to Q^4 sites where the SiO_4 tetrahedra are linked with four other SiO_4 tetrahedra. In the Laponite clay structure, there should be no Q^4 sites,[8,32] and this is confirmed by the spectrum of the clay. Thus, the Q^4 sites have resulted from the profound structure changes of the silicate in the synthesis.

These results suggest that the clay layers could be seriously attacked if the acidity of the precursor solution is strong. On the other hand, the Laponite dispersion with a high pH (∼10) inevitably induces further hydrolysis of the metal hydroxyl oligomers in the precursor solution, forming larger species, the precursors of metal oxide nanoparticles. These large species most likely condense to the surrounding silicate fragments because they carry opposite electric charges. This leads to a composite structure in which the metal oxide particles of several nanometers in size are dispersed among the silicate media.

The metal oxide in these mesoporous composites could be distinctly different from that in their pillared clay counterparts. We can see the aggregation of crystallites between 3 and 10 nm in the TiO_2−nanocomposite (Figure 1b), which are anatase crystals with a mean crystal size of 5 nm, according to the XRD pattern of the sample powder. The acid leaching was also observed for other metal oxide composites. However, the leaching extent is different from sample to sample (Table 1) because the acidities of the precursor solutions are different. For instance, the acidity of the precursor for the TiO_2−composite is similar to that of 1 M [H^+] solution, while those for the CeO_2/Al_2O_3−composite and La_2O_3/Al_2O_3−composite have a pH of about 3. Chemical compositions at different particles of a sample were analyzed on TEM by the EDS technique. All sample grains analyzed, even as small as 30 nm in size, contained silicon and the metal elements introduced. Metal oxide and leached silicate nanoparticles are two interdispersed phases forming mesoporous composite structures, and a large surface area of the metal oxide is available for the reactant molecules.

The decisive issue in creating a mesoporous composite structure is to polymerize the oligomers to the species several nanometers in size after they are dispersed within the interlayer space rather than precipitating alone. The hydrate cations of many metal elements are stable only in an acidic environment.[2,19] If the pH increases, the metal hydrate ions hydrolyze, forming polymerized hydroxyl ions, and finally precipitate. The dispersion of Laponite has a pH value of about 10, which inevitably induces further hydrolysis of the metal hydrate species when the two were mixed, forming larger species that are the precursors of metal oxide nanoparticles. These large species most likely condense to the surrounding silicate fragments, which are the residues of leached Laponite. In this study, the hydrolysis of metal hydrate poly cations and acid leaching of clay layers are coupled, resulting in highly porous solids of metal oxides and silicate particles. The composites thus obtained possess several important advantages. The metal oxides exist in individual fine crystals of several nanometers, having a large specific surface area that is accessible to the reactant molecules. This is crucial for the catalytic applications.[1,15] The presence of the silicate fragments in the samples prevents the nanoparticles of metal oxide from sintering when they

(32) Wilson, M. A. *NMR Techniques and Applications in Geochemistry and Soil Chemistry*; Pergamon Press: Oxford, 1987.

Table 2. Specific Surface Area (BET S.A.) and Pore Volume (V_p)[a] of Some Composites of Metal Oxide and Silicate (Calcined at 773 K)

	prepared with PEO		prepared without PEO	
metal oxide	BET S.A. (m^2/g)	V_p (cm^3/g)	BET S.A. (m^2/g)	V_p (cm^3/g)
TiO_2−C	635	0.776	343	0.405
Cr_2O_3−C	894	1.124	679	0.461
Fe_2O_3−C	434	0.547	419	0.307
NiO−C	356	0.681	245	0.174
Mn_3O_4−C	481	0.754	355	0.276
ZrO_2−C	459	0.430	248	0.146
CeO_2/ZrO_2−C	611	0.676	291	0.185
Al_2O_3/La_2O_3−C	587	0.676	439	0.383
Al_2O_3/CeO_2−C	599	0.775	422	0.345

[a] The specific surface area and pore volume were calculated using nitrogen sorption data.[6]

are heated at high temperatures during the synthesis and applications. The structures have a much larger pore volume and pore size, as compared to pillared clays, and the mesoporous structure is stable because of its composite structures. Consequently, these composites are expected to be superior catalysts.

As illustrated in Table 2, the calcined composite samples exhibit much larger surface areas and pore volumes as compared to corresponding pillared layered clays (pore volume of 0.15−0.40 cm^3/g and BET surface area 150−400 m^2/g).[4−7,9−14,16] For instance, the mixed oxide pillared clay La_2O_3/Al_2O_3 pillared montmorillonite has a BET surface area of 321 m^2/g and pore volume of 0.18 cm^3/g,[16] while the BET surface area and pore volume of the La_2O_3/Al_2O_3−composite of 439 m^2/g and 0.383 cm^3/g (Table 2), respectively. For the La_2O_3/Al_2O_3−composite prepared with a PEO surfactant, they are even remarkably larger: 587 m^2/g and 0.676 cm^3/g, respectively.

Besides, the porosity of the nanocomposite can be significantly increased by introducing poly(ethylene oxide) (PEO) surfactants. A certain amount of a PEO surfactant could be added into the Laponite dispersion prior to introducing the precursor solution. These surfactants have strong affinities to the surfaces of clay and metal hydrates, preventing the metal hydrate species from further agglomeration during the drying and heating processes. After the composite structures are solidified, the surfactant molecules were evaporated at temperatures between 473 and 523 K, leaving numerous pores in the structure. We observed that the surfactant evaporated and that the surfactant liquid condensed outside of the furnace. On the other hand, the affinity of the surfactant molecules to the metal hydrate particles is different from metal to metal. This may explain that the effect of adding PEO could be substantially different from one composite to another as shown in Table 2. The nitrogen sorption isotherms of the CeO_2/Al_2O_3–composite samples prepared with and without PEO surfactant, respectively, are illustrated in Figure 4 (as representatives). As can be seen, the nitrogen adsorption capacity of the sample prepared with PEO is more than twice of the capacity of the sample prepared. The capacity of a solid reflects the pore volume in the solid.[26] Therefore, the pore volume of the CeO_2/Al_2O_3−composite can be doubled by the use of the PEO surfactant in the synthesis.

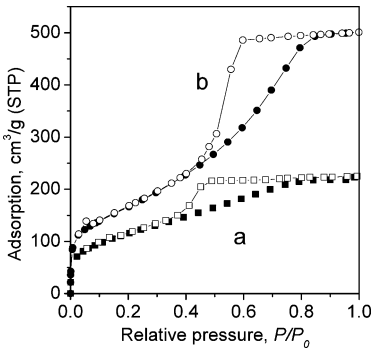

Figure 4. Nitrogen sorption isotherms of the CeO_2/Al_2O_3−composite samples prepared without (isotherm a) and with PEO surfactant (isotherm b). The solid marks are for adsorption data and empty ones for desorption data.

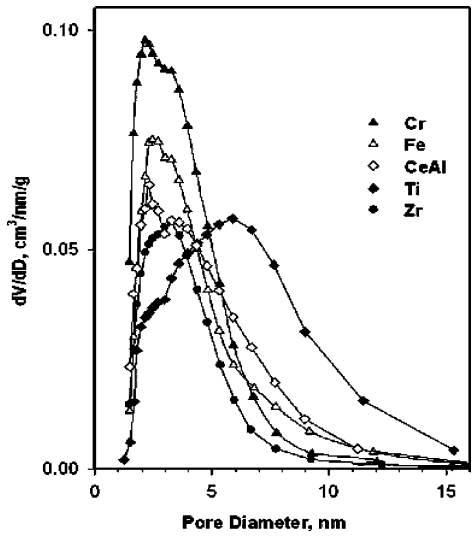

Figure 5. PSDs of the samples. The metal element introduced in the synthesis is used to indicate the PSD of the obtained sample.

The pore size distributions (PSDs) of five samples are illustrated in Figure 5. The PSDs were calculated from nitrogen physical sorption data.[27] Most pores in the Cr_2O_{3-}, Fe_2O_{3-}, ZrO_{2-}, and mixed oxide CeO_2/Al_2O_{3-}composite samples are in a range between 2 and 8 nm. The PSD of TiO_{2-}composite is broader than the others.

It is known that in templated synthesis, the pore size of the product is proportional to the molecular size of the surfactant.[21,33−35] But, there is no such trend observed in this study. The molecular size of the surfactant is not a sole determinant of the pore size of the product solids. The PEO surfactant acts as a spacer creating porosity in the inorganic solids.[36]

When other parameters in the synthesis were kept constant, the size and volume of the mesopores in the samples varied with the amount of PEO: an increase to a maximum and a slight decrease as the PEO amount increased further. During heating, the surfactant volatilizes, leaving a rigid structure with high porosity. The pore size distributions (PSDs) of

(33) Kresge, A. C. T.; Leonowicz, M. E.; Roth, W. J.; Vartuli, J. C.; Beck, J. S. *Nature* **1992**, *359*, 710.
(34) Inagaki, S.; Fukushima, Y.; Kuroda, K. *J. Chem. Soc., Chem. Commun.* **1993**, 680.
(35) Zhao, D.; Feng, J.; Huo, Q.; Melosh, N.; Fredrickson, G. H.; Chmelka, B. F.; Stucky, G. D. *Science* **1998**, *279*, 548.
(36) Sieg, R. P. Catalysts. U.S. Patent 2,697,066, 1954.

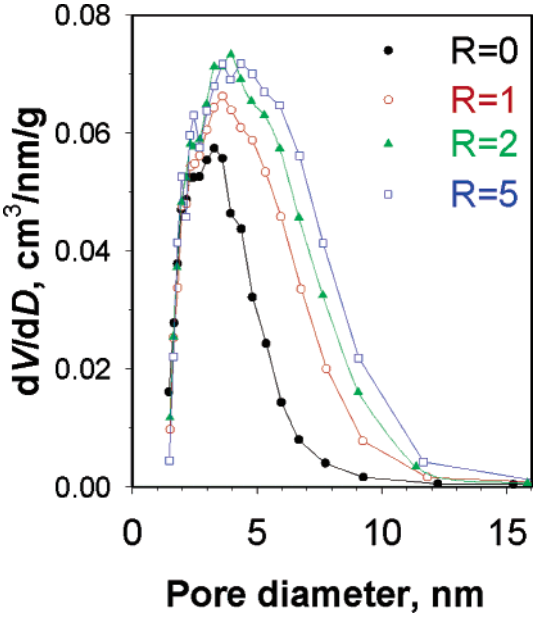

Figure 6. PSDs of the ZrO_2−composite. R is the ratio of PEO amount to Laponite amount, which was 4.0 g for all the samples in the figure. The PEO amount varies from 0 to 20 g.

Scheme 1. Schematic for Formation of Mesoporous Nanocomposites from a Laponite Suspension and Aqueous Solution of a Metal Salt[a]

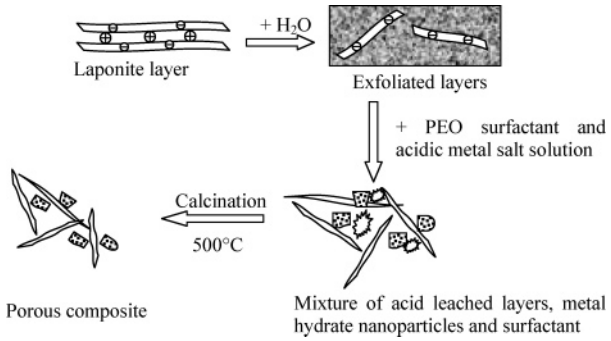

[a] PEO surfactant is added to increase the porosity of the composite. Dotted particles are metal oxide.

ZrO_2−composites prepared with various amounts of a PEO surfactant, $C_{12-14}H_{25-29}O(CH_2CH_2O)_7H$, are shown in Figure 6. As the amount of PEO used increased while other parameters in the synthesis were kept constant, the PSD peak shifted to large pores and became broader. The total pore volume also increased with the PEO amount. These findings allow us to effectively tailor the structure of these solids for various applications.

The general process for the formation of the mesoporous composites of metal oxide and silicate (from leached clay layers) nanoparticles is summarized in Scheme 1. It indicates schematically the Laponite exfoliation in water, acid leaching of the clay, and function of the PEO surfactant as a spacer.

During the last two decades, the potential application of pillared clays as catalysts or catalyst supports for numerous chemical reactions has been attempted.[37−41] In general, better

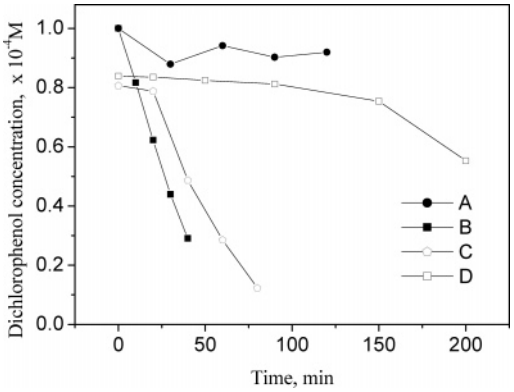

Figure 7. Catalytic performance of the samples for photodegradation of 2,4-dichlorophenol. Curve A is the blank. Curves B−D illustrate the performance of the ultra-fine TiO_2 powder P25, a TiO_2−composite sample, and TiO_2−pillared clay, respectively.

acidic characteristics, larger specific surface areas, pore volumes, and pore sizes are required for catalysis purposes. The composites in this study are remarkably superior, in terms of these properties, to the pillared clays. The TiO_2−composites prepared in this study were used as photocatalysts for photodegradation of a synthetic dye (Rhodamine 6G) and a phenol (2,4-dicholorophenol). For photodegradation of the synthetic dye, the UV source was a 100 W Hg lamp (Toshiba SHLS-1002A). Aqueous suspensions of Rhodamine 6G (25 mL, with an initial concentration of 2×10^{-5} M) and a photocatalyst powder (25 mg) were placed in a Pyrex vessel. Prior to irradiation, the suspensions were magnetically stirred in the dark for ca. 30 min to establish an adsorption/desorption equilibrium between the dye and the catalyst surface. At given intervals of illumination, a specimen of the suspension was collected and analyzed by UV−vis spectroscopy using a lambda Bio 20 spectrophotometer. For the photodegradation of 2,4-dicholorophenol, the UV source was four 8 W light tubes that could emit light with a wavelength of 356 nm. The initial concentration of the phenol was 10 ppm, and the concentration of the catalyst was 1 g/L. The activity was expressed as the decrease in phenol concentration with time, which was analyzed by colorimetric methods.[42]

The overall photocatalytic efficiency of a TiO_2−composite is significantly better than that of the pillared clay, while the TiO_2 content in two samples is similar (Figure 7).

In the mesoporous composite structure, TiO_2 exists in anatase nanoparticles, and the anatase phase is known as the most active TiO_2 phase, while most of the TiO_2 pillars between the clay layers are too small to form crystallites. The XRD patterns of the TiO_2–composite and TiO_2–pillared montmorillonite are illustrated in Figure 8. The intensity of the diffraction peaks from the anatase phase in the TiO_2–composite is much stronger than that in the pillared

(37) Carrado, K. A.; Suib, S. L.; Skoularikis, N. D.; Coughlin, R. W. *Inorg. Chem.* **1986**, *25*, 4217.
(38) Comets, J. M.; Chen, X.; Kevan, L. *J. Phys. Chem.* **1993**, *97*, 8646.
(39) Kostapapas, A.; Suib, S. L.; Coughlin, R. W.; Occelli, M. L. In *Zeolites: Facts, Figures, Future*; Jacobs, P. A., Van Santen, R. A., Eds.; Elsevier Science Publishers B. V.: Amsterdam, 1989; p 399.
(40) Lenarda, M.; Ganzerla, R.; Storaro, L.; Enzo, S.; Zanoni, R. *J. Mol. Catal.* **1994**, *92*, 201.
(41) Occelli, M. L.; Dominguez, J. M.; Eckert, H. *J. Catal.* **1993**, *141*, 510.
(42) Ettinger, M. B.; Ruchhoft, C. C.; Lishka, R. J. *Anal. Chem.* **1951**, *23*, 1783.

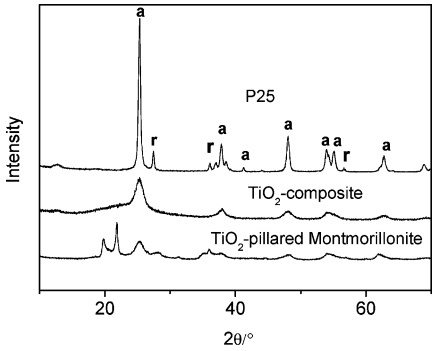

Figure 8. XRD patterns of P25, TiO_2−composite, and TiO_2−pillared montmorillonite. The intensities of the diffraction peaks from the anatase phase (labeled with letter a) of the TiO_2−composite are remarkably higher than those in TiO_2−pillared montmorillonite, indicating better crystallinity of anatase in the TiO_2−composite sample.

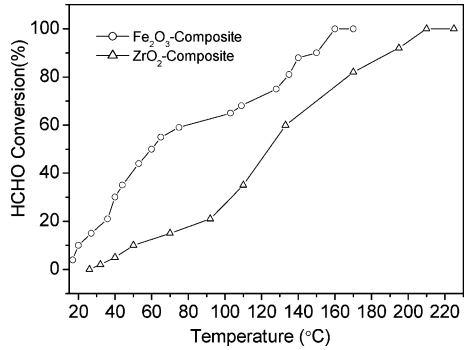

Figure 9. Catalytic oxidation of formaldehyde on the catalysts of gold supported on Fe_2O_3−composite and ZrO_2−composite.

clay (Figure 8), indicating better crystallized anatase in the TiO_2–composites. For comparison, the pattern of the well-known titania powder P25 (a mixtured powder of ∼80% anatase and ∼20% rutile) from Degussa is also given in Figure 8.

The photoactivity of the TiO_2−composite is comparable to P25 (Figure 7), but the TiO_2 content in the composite is about 44% (Table 1). The activity per unit of TiO_2 in the composite is even better than that of P25. This could be attributed to the smaller anatase crystal size and thus larger specific surface area of anatase in the composite. The mean size of the anatase crystals in this sample is 5.0 nm (this is calculated from the XRD pattern in Figure 8 using the Scherrer equation). The particle size of P25 is about 30−50 nm, and the specific surface area of the powder is about 40 m^2/g. The P25 particles consist of anatase and rutile crystals, and the mean size of the anatase crystals is 18.3 nm derived from the XRD pattern in Figure 8 using the Scherrer equation.

Moreover, the composite retains the feature of TiO_2−pillared clay, which can be recovered readily from water after use. The ultrafine powders, like P25, exhibit a superior activity because of the large surface-to-volume ratio. However, it is extremely difficult to recover them from water after they are used in aqueous systems, leading to a potential difficulty in downstream separation. In fact, the high cost for separating the catalyst nanocrystals has seriously impeded the applications of TiO_2 photocatalysts at industrial scales.[43,44] In the nanocomposites of the present study, the metal oxide nanocrystals, such as anatase nanocrystals (shown in Figure 1b), are linked by the silicate, forming porous aggregates with sizes at the micrometer scale. These aggregate particles can be readily separated from water by filtration or sedimentation. Developing recyclable photocatalysts is of great significance for their application as photocatalysts for the elimination of organic pollutants from water at an industrial scale.

One important feature of layered clay materials is their ion exchange ability, which is useful for introducing ionic catalytic active components into the porous systems.[12,13] We found that the cation exchange capacity of ZrO_2−composites can be considerably enhanced by treatment with a diluted NaOH solution, similar to that observed in conventional pillared clays.[12,13] For instance, the amount of gold loaded onto the composite increases from 0.25 to 0.85 wt % by treatment with the NaOH solution. A catalyst of 0.80 wt % of gold loaded on a ZrO_2−composite can completely oxidize formaldehyde HCHO to carbon dioxide at 208 °C.

Such a HCHO oxidation on the gold catalyst on an Fe_2O_3−composite, in which 0.90 wt % gold was loaded by ion exchange, takes place at as low as 17 °C and achieves 100% conversion from HCHO to CO_2 at 160 °C (Figure 9).

The large surface area and cation exchange property of the mesoporous composite support allow gold to exist in a well-dispersed form, providing numerous active sites for the catalytic reaction. Such a catalyst has a high activity even in a situation with a large moisture content. Finally, these nanocomposite solids can be readily granulated to designed shapes, and the grains have good strength. These findings shed light on the potential of metal oxide composites as advanced catalysts.

Conclusion

In summary, we have proposed a general synthesis strategy for constructing highly porous composite structures of metal oxide and silicate nanoparticles from aqueous systems. In this approach, the reaction between the Laponite clay and the precursor solution of metal oxides (the pillaring solution) is intensified by aging at 100 °C for 2 days. Such a synthesis involves two coupled processes: leaching the clay layers of Laponite and further hydrolysis of the metal hydrate species. The latter leads to the formation of larger species that are converted into metal oxide nanoparticles in the subsequent calcination. The extent of the acid leaching varies from precursor to precursor. For the precursors of strong acidity, the clay platelets are acid leached and converted to amorphous silicate fragments and the precursors of metal oxide nanoparticles condensed on the silicates, forming mesoporous composite structures. For other precursors, the acid leaching is not serious so that the clay layer structure is retained, and mesoporous composite structures of metal oxide nanoparticles and clay layers can be obtained (for example, Mn_3O_4−nanocomposite). Introducing PEO surfactants in the synthesis leads to increases in both the specific surface area and the

(43) Hoffmann, M. R.; Martin, S. T.; Choi, W.; Bahnemannt, D. W. *Chem. Rev.* **1995**, *95*, 69.
(44) Beydoun, D.; Amal, R.; Low, G. K.-C.; McEvoy, S. *J. Phys. Chem. B* **2000**, *104*, 4387.

pore volume of the calcined products, and the increase is considerable for some samples. According to this mechanism, we can alter the particle size of the metal oxides by manipulating the acidity of the precursor solution. With smaller sizes of metal oxide crystals, a larger porosity, ion exchange capacity, and readiness for granulation these nanocomposites are superior as photocatalysts and catalyst supports. The proposed synthesis is an effective approach for constructing nanocomposites witha large porosity and structure and surface chemistry that can be tailored.

Acknowledgment. Financial support from the Australian Research Council (ARC) and National Science Foundation of China (20263001) is gratefully acknowledged.

Supporting Information Available: Dark-field images and XRD patterns of some composite samples in PDF format. This material is available free of charge via the Internet at http://pubs.acs.org.

CM060390+